

## GEOTECHNICAL AND GEOPHYSICAL TESTS FOLLOWING THE 2020 EARTHQUAKE-INDUCED LIQUEFACTION PHENOMENA

Sara Amoroso<sup>(1)</sup>, Kyle M. Rollins<sup>(2)</sup>, Giuseppe Di Giulio<sup>(3)</sup>, Lara Wach<sup>(4)</sup>, Kosta Urumović<sup>(5)</sup>, Diana Faieta<sup>(6)</sup>, Radovan Filjak<sup>(7)</sup>, Daniela Fontana<sup>(8)</sup>, Stefano Lugli<sup>(9)</sup>, Maria Manuel<sup>(10)</sup>, Giuliano Milana<sup>(11)</sup>, Luca Minarelli<sup>(12)</sup>, Marko Budić<sup>(13)</sup>, Nikola Belić<sup>(14)</sup>, Tomislav Kurečić<sup>(15)</sup>, Luka Sorić<sup>(16)</sup>, Marco Stefani<sup>(17)</sup>, Gabriele Tarabusi<sup>(18)</sup>, Maurizio Vassallo<sup>(19)</sup>

<sup>(1)</sup> Associate Professor, University of Chieti-Pescara, Italy; Research Associate, Istituto Nazionale di Geofisica e Vulcanologia, Italy, [sara.amoroso@unich.it](mailto:sara.amoroso@unich.it)

<sup>(2)</sup> Full Professor, Brigham Young University, Utah, USA, [rollinsk@byu.edu](mailto:rollinsk@byu.edu)

<sup>(3)</sup> Researcher, Istituto Nazionale di Geofisica e Vulcanologia, Italy, [giuseppe.digiulio@ingv.it](mailto:giuseppe.digiulio@ingv.it)

<sup>(4)</sup> Researcher, Croatian Geological Survey, Croatia, [lwacha@hgi-cgs.hr](mailto:lwacha@hgi-cgs.hr)

<sup>(5)</sup> Researcher, Croatian Geological Survey, Croatia, [kurumovic@hgi-cgs.hr](mailto:kurumovic@hgi-cgs.hr)

<sup>(6)</sup> Master Student, University of Chieti-Pescara, Italy, [diana.faieta@studenti.unich.it](mailto:diana.faieta@studenti.unich.it)

<sup>(7)</sup> Researcher, Croatian Geological Survey, Croatia, [rfiljak@hgi-cgs.hr](mailto:rfiljak@hgi-cgs.hr)

<sup>(8)</sup> Full Professor, University of Modena and Reggio Emilia, Italy, [daniela.fontana@unimore.it](mailto:daniela.fontana@unimore.it)

<sup>(9)</sup> Associate Professor, University of Modena and Reggio Emilia, Italy, [stefano.lugli@unimore.it](mailto:stefano.lugli@unimore.it)

<sup>(10)</sup> Owner and Chief Geologist, Geo Geotecnica e Geognostica s.r.l., Italy, [maria.manuel.geo@icloud.com](mailto:maria.manuel.geo@icloud.com)

<sup>(11)</sup> Technologist, Istituto Nazionale di Geofisica e Vulcanologia, Italy, [giuliano.milana@ingv.it](mailto:giuliano.milana@ingv.it)

<sup>(12)</sup> Research Fellow, Istituto Nazionale di Geofisica e Vulcanologia, Italy, [luca.minarelli@ingv.it](mailto:luca.minarelli@ingv.it)

<sup>(13)</sup> Researcher, Croatian Geological Survey, Croatia, [mbudic@hgi-cgs.hr](mailto:mbudic@hgi-cgs.hr)

<sup>(14)</sup> PhD Student, Croatian Geological Survey, Croatia, [nbelic@hgi-cgs.hr](mailto:nbelic@hgi-cgs.hr)

<sup>(15)</sup> Researcher Croatian Geological Survey, Croatia, [tkurecic@hgi-cgs.hr](mailto:tkurecic@hgi-cgs.hr)

<sup>(16)</sup> Owner and Chief Engineer, Geotehnički studio d.o.o., Croatia, [Luka.Soric@geotehnicki-studio.hr](mailto:Luka.Soric@geotehnicki-studio.hr)

<sup>(17)</sup> Associate Professor, University of Ferrara, Italy, [marco.stefani@unife.it](mailto:marco.stefani@unife.it)

<sup>(18)</sup> Technologist, Istituto Nazionale di Geofisica e Vulcanologia, Italy, [gabriele.tarabusi@ingv.it](mailto:gabriele.tarabusi@ingv.it)

<sup>(19)</sup> Researcher, Istituto Nazionale di Geofisica e Vulcanologia, Italy, [maurizio.vassallo@ingv.it](mailto:maurizio.vassallo@ingv.it)

### Abstract

Earthquakes and related coseismic effects at the surface, such as liquefaction and lateral spreading, can impact humans due to the resulting economic or social disruptions (e.g. slope and foundation failures, flotation of buried structures, etc.). In this respect, the 2020 Petrinja  $M_w$ 6.4 earthquake (Croatia) provided many examples of liquefaction and lateral spreading, as identified by the post-earthquake field reconnaissance campaigns. The observed liquefaction cases occurred in the alluvial plains of the Kupa, Sava and Glina Rivers or along faults, with ejecta composed of sands and/or gravels of different grain size and mineralogy. The lateral spreading phenomena were observed along river embankments and roads. In this context interest in studying these different features arose, and an international research team from Italy, the United States and Croatia recently performed an intensive geological, geotechnical and geophysical campaign to assess the liquefaction susceptibility at selected sites located throughout the epicentral area (from Glina to Petrinja to Sisak). Innovative in-situ test equipment, such as the dynamic cone penetration test (DPT) for liquefied gravels and the Medusa flat dilatometer test (Medusa DMT) for liquefied sands, were employed in combination with standard in-situ tests, such as the standard penetration test (SPT), the piezocone test (CPTU), and shear wave velocity ( $V_s$ ) measurements. These techniques were employed to verify their advantages relative to the existing liquefaction triggering charts and to characterize the soil properties of the buried liquefied layers and the non-liquefied crust. This paper presents preliminary results and comparisons at some of the investigated liquefaction sites.

*Keywords: liquefaction, in-situ geotechnical and geophysical tests, dynamic cone penetration test, medusa flat dilatometer test, 2020 Petrinja  $M_w$ 6.4 earthquake (Croatia).*

## 1. Introduction

Earthquakes and related phenomena, such as liquefaction-triggered lateral spreading, can generate important economic or social disruptions. It is therefore necessary to adopt proactive measures to manage earthquake risk by ground strengthening to prevent slope and foundation failures, and flotation of buried structures, as stated in several building codes (e.g. [1]). In this respect, the collection of field data regarding liquefaction phenomena is critical to improving knowledge on ground failures and impacts to man-made structures.

The 2020 Petrinja  $M_w6.4$  earthquake (Croatia) provided many examples of liquefaction and lateral spreading, as identified by the post-earthquake field reconnaissance campaigns and by remote surveys using drone photos [2, 3]. In this context, interest in studying such different features arose, and an international research team from Italy, the United States and Croatia began an intensive geological, geotechnical and geophysical campaign beginning in September 2022 which is still ongoing. This study is using innovative in-situ techniques and equipment to assess the liquefaction susceptibility at ten selected sites throughout the epicentral area (between Glina, Petrinja and Sisak; Fig. 1). The objectives were to verify their advantages relative to the existing liquefaction triggering charts and to characterize the properties of the liquefied deposits and the non-liquefied crust. This paper describes the field tests, and presents some preliminary results and comparisons at some of the investigated liquefaction sites.

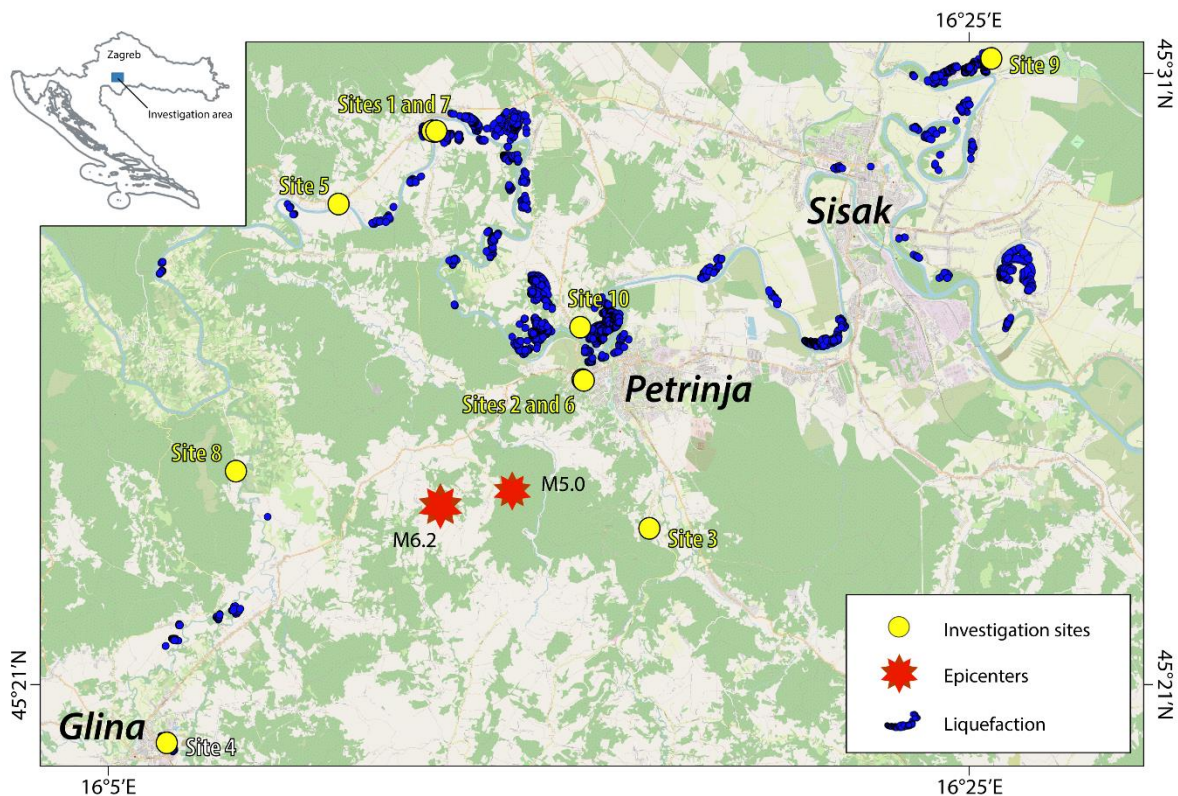


Figure 1. Location of the field investigation sites and epicenters of the 2020  $M_w6.4$  and  $M_w5.0$  Petrinja earthquakes with OpenStreetMap as background [2]. The locations of the observed liquefaction manifestations were derived from drone images taken by HGI and available satellite images.

## 2. Geological setting

The earthquake-affected area [4] is located in the continental part of Croatia (Fig. 1), at the southwestern margin of the Sava Basin within the Pannonian Basin System. The wide Petrinja region is located between the Adria-derived units of the Dinarides to the southwest, and the Europe-derived

units (Tisza mega unit) of the Pannonian region to the northeast [2, 5]. During the Tertiary, the region was subjected to tectonic extension (Miocene), followed by a compressional phase (Pliocene-Quaternary), eventually generating a complex framework of NW-SE striking, inverted normal faults [6, 7]. The epicentral area of the 2020 earthquake is located in the Hrastovička mountain, composed of various basement rocks (Jurassic-Paleogene) such as metamorphites of the ophiolitic complex, volcanic rocks, spilites, marine limestone, turbiditic calcarenites, marls conglomerates, sandstones, shales and coals [8, 9]. The liquefaction phenomena occurred in the lowlands at elevations between 100 and 200 m (Fig. 1). The Neogene and Quaternary deposits form the sedimentary infill of the Pannonian Basin System [10]. Some of the coseismic effects were recorded within the Neogene bioclastic limestones and calcrudites, but most of them occurred in the alluvial plains of Glina, Kupa, and Sava Rivers. The affected sediments were deposited in different environments such as flood plain, meander oxbow, and active streams. The liquefaction affected lithologies widely vary from clays, to silts, sands, and gravels, although the silty sediments are prevailing. the overall thickness of the Quaternary succession is usually up to 5 m in alluvial plains, but it may reach estimated at a maximum of up to 30 m [8, 9].

### **3. The 2020 Petrinja earthquake**

#### **3.1 Seismic event**

On 29<sup>th</sup> December 2020 at 11:19 (UTC), the town of Petrinja and its surroundings were hit by a destructive  $M_w$ 6.4 earthquake [11]. The seismic sequence began in the morning of the previous day (05:28 UTC) with  $M_w$ 5.0 earthquake centered about 5 km southwest of Petrinja [2]. According to [11] and the Croatian Earthquake Catalogue – CEC (updated and continuously supplemented version first described in [12]), the mainshock was with a shallow crustal depth of about 6 km, generating moderate to strong shaking in central Croatia, and was largely felt across Croatia and neighbouring countries. Earthquake shaking triggered surface ruptures along the fault trace, and extensive liquefaction and lateral spreading within approximately 20 km around the epicentre (Fig. 1) [2, 3]. Based on its surface projection and orientation, the ruptured zone was associated to the Petrinja-Pokupsko Fault (PPKF). Following the NW-SE orientation of the older faults, the PPKF most probably represents a re-activated deep-seated dextral strike-slip fault zone [2].

#### **3.2 Liquefaction evidences**

An European team of researchers (geologists and engineers), in tight collaboration with the Croatian Geological Survey, performed field reconnaissance campaigns with the aim of providing a detailed identification and characterization of the primary and secondary geological and geotechnical coseismic effects induced by the Croatian earthquakes [2]. To improve the understanding of the liquefaction phenomena [3], the Working Group integrated the data collected directly in the field with those from a remote survey by drone aerial photos acquired immediately following the earthquakes. This process allowed for the collection of the liquefaction record with the highest possible completeness both in terms of pattern and distribution of the phenomena. The data set includes several detailed case studies typified by the following characteristics: (a) liquefaction occurring on alluvial plain sites (Kupa, Sava and Glina rivers); (b) ejecta consisting of sand and/or gravel locally associated with shells and armoured mud balls; (c) lateral spreading phenomena along roads and river embankments; (d) sand ejecta of different grain size and composition, even at the same site; and (e) sand and/or gravel ejecta developed along fault traces.



Figure 2. Examples of liquefaction following the Petrinja earthquake (modified after [2]): a) lateral spreading along Kupa river embankment at Letovanic; b) crack with sand ejecta in the alluvial plain of the Sava river; and c) sand and gravel ejecta of different provenance with the presence of shells close to the Kupa river.

## 4. Site investigations

At the ten research sites, a thorough geological, geotechnical and geophysical site investigation was planned using innovative in-situ test equipment, as described in the following paragraphs. Most of the investigations were carried out in September 2022, although some of them are still ongoing due to weather conditions and flooding near the rivers. At each of the six gravel sites, dynamic cone penetration (DPT) tests were performed in combination with boreholes, piezocone test (CPTU), and shear wave velocity ( $V_s$ ) measurements. At the lateral spreading site, boreholes with standard penetration tests (SPT) at approximately 0.5-meter intervals were performed. Finally, at the liquefied sandy sites with high fines content, the Medusa flat dilatometer test (Medusa DMT) was employed in combination with standard geotechnical in-situ tests, such as borehole with SPTs, CPTU and  $V_s$  measurements. Currently, laboratory analyses are being conducted on soil samples collected at all sites to provide information on mineralogy and geotechnical properties of the liquefied sandy and gravelly deposits and of the non-liquefied crusts.

### 4.1 Dynamic cone penetration test (DPT)

The dynamic cone penetration test (DPT) was developed in China in the early 1950s to measure penetration resistance of gravel for application in bearing capacity analyses. Based on their experience, standard test procedures and code provisions have been formulated [13, 14]. Because of widespread gravelly deposits beneath the Chengdu plain, the DPT is widely used in that region, particularly for the evaluation of liquefaction potential [15]. More recently, an updated liquefaction triggering curve has been proposed by [16] using a worldwide database.

DPT equipment is relatively simple, consisting of a 120-kg hammer, raised to a free fall height of 100 cm, then dropped onto an anvil attached to 60-mm diameter drill rods which in turn are attached to a solid steel cone tip with a diameter of 74 mm and a cone angle of 60° as shown in Fig. 3a. The larger cone makes it less affected by gravel particles, while the smaller rod diameter helps to reduce shaft friction on the rods behind the cone tip.

Prior to testing, the drill rods are marked at 10 cm intervals (see the detail in Fig. 3b, photo of the Petrinja DPT test) and the number of blows required to penetrate each 10 cm is recorded. The raw DPT blow count is defined as the number of hammer drops required to advance the cone tip 10 cm. A second penetration resistance measure, called  $N_{120}$ , is specified in Chinese code applications where  $N_{120}$  is the number of blows required to drive the cone tip 30 cm; however,  $N_{120}$  is calculated simply by multiplying raw blow counts by a factor of three which preserves the detail of the raw blow count record.

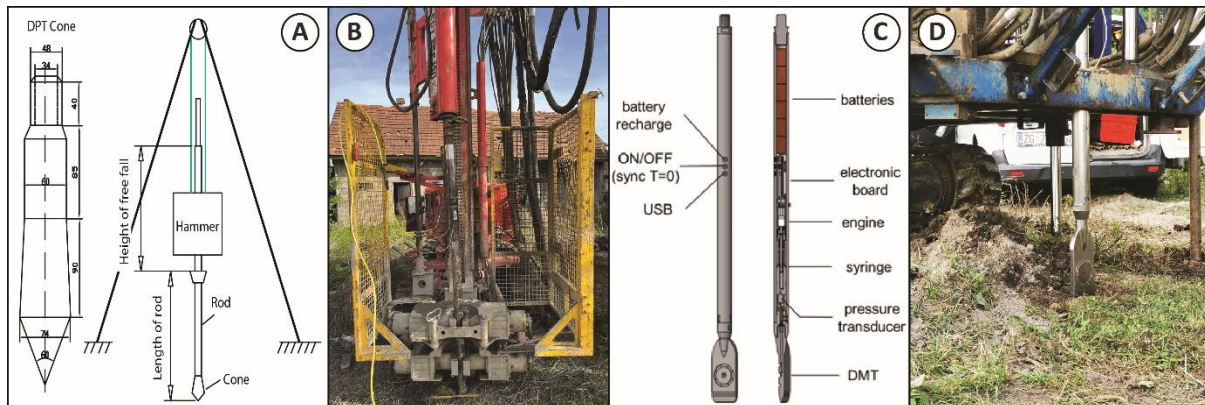


Figure 3. a) Component sketch of tripod and drop hammer setup for dynamic penetration tests (DPT) along with DPT cone tip (modified after [15]); b) photo of DPT testing at one of the Croatian site investigation with conventional drill rig; c) Medusa DMT layout [17]; d) photo of the Medusa DMT testing at one of the Croatian site investigation using a conventional light penetrometer combined with drill rig.

#### 4.2 Medusa dilatometer test (Medusa DMT)

The Medusa DMT is the combination of a flat dilatometer with a hydraulic automation and measuring system for autonomously performing DMT tests [17]. Fig. 3 shows the main components of the instrument, together with a photo of a Medusa DMT test performed in September 2022 in Croatia. A rechargeable battery pack powers an electronic board, connected to a pressure transducer and to a custom-designed motorized syringe. The firmware coded in the electronics activates the motorized syringe for generating the pressure required to obtain the DMT readings. The maximum operating pressure is 25 MPa. A high accuracy pressure transducer is used to measure the pressure generated by the syringe and operating on the membrane. An electric wire provides the contact status of the membrane to the electronic board. The A, B, and C pressure readings are taken by the electronics firmware with the same criteria used for the traditional pneumatic DMT equipment. Details on calibration chamber and field validation of the Medusa DMT can be found in [17, 18, 19, 20].

#### 4.3 Geophysical surveys (H/V and surface-wave analysis)

To better reconstruct the near-surface velocity profile an extensive geophysical survey was carried out using both two-dimensional (2D) arrays of seismic nodes and linear array of geophones. For the 2D array, a quite innovative technology in small-scale surveys based on seismic nodes was used [21, 22]. Seismic nodes are composed of compact digitizers with internal battery connected to 3C geophones (GSB-3C and GS-one manufactured by Geospace Technologies), and the absence of cable and their ease in the field installation allowed to quickly deploy a large number of nodes (from 20 to 46 depending on site). Seismic nodes were arranged at each selected site in a circular geometry (Table 1) with usually 3 circular rings with different radius (about 5, 12 and 25 m), and a node in the centre close to DPT or Medusa DMT surveys. Seismic nodes recorded at each site a few hours of ambient vibrations (seismic noise) with a sampling rate that was set equal to 250 Hz.

From seismic noise data collected by 3C nodes, it was possible to compute the horizontal-to-vertical noise spectral ratio (H/V curve), and derive the site resonance frequency ( $f_0$ ) from the peak in the H/V curve [23].  $f_0$  is an important proxy for potential site amplification [24] used in site characterization analyses and microzonation mapping. It is related to the presence of a strong seismic impedance contrast in the subsoil profile, where  $f_0$  value is linked to the average thickness and shear-wave velocity of soft soil deposits overlaying a stiffer soil unit or bedrock interface [25].

For the linear array of geophones, a maximum of 72 vertical geophones (eigen-frequency 4.5 Hz) connected to a multi-channel acquisition system was used (Geode manufactured by Geometrics, connected in serial for a maximum number of 3 Geode) recording files with length of 1.5 s and sampling rate equal to 8000 Hz. The 72 geophones were equally spaced from 0.5 to 1 m, depending

on the site (Table 1). In contrast to the 2D array of nodes which collects seismic noise, the linear array records seismic signals produced by an active source composed of a 5 kg-sledge-hammer hitting a metal plate. The seismic source was located at the beginning, in the middle and at the end of the linear array of geophones in order to reproduce forward and reverse shot records.

To provide absolute positions for each seismic measurement, a real-time kinematic (RTK) positioning was used through a GNSS receiver (S900a new manufactured by Stonex). In this way, the position of each deployed node and the first and last geophones within the 1D line were measured with accuracy of a few cm. The absolute position was also measured for the geotechnical and borehole surveys previously discussed. In order to derive a surface-wave dispersion curve, active data collected by the linear geophones array and passive data from nodes will be analysed with the multichannel analysis of surface waves (MASW) technique [26, 27]. In particular, the analysis from 3-components data recorded by nodes will allow to retrieve the Rayleigh and Love dispersion curves.

The surface-wave dispersion curves obtained by 1D active array and 2D passive array will be combined to achieve information in a large frequency band. In general, active methods provide results at higher frequencies in comparison to passive techniques [28]. However, in the analysed experiment the dispersion curves are expected to extend toward high frequencies also in the passive case, due to the large number of seismic nodes deployed in a relatively small area (Table 1).

Table 1 – Geophysical surveys performed at the selected sites. For the position of the Site, refer to Fig. 1. For Sites 2 and 6, the geometry of array installation is reported in Fig. 6

ID site	Date of geophysical survey	2D arrays: number of seismic GSB nodes (and radius with maximum aperture)	1D array using 72 vertical geophones: spacing between adjacent geophone
Site 1	14 September 2022	32 (25 m)	1 m
Site 2	12 September 2022	46 (21 m); array A in Fig. 6	0.5 m
Site 3	13 September 2022	26	0.5 m
Site 4	15 September 2022	29 (22 m)	1 m
Site 5	14 September 2022	-	0.5 m
Site 6	15 September 2022	20 (10 m) array F in Fig. 6	-
Site 10	16 September 2022	25 (20 m)	-

## 5. Preliminary results

Considering that the field campaign is ongoing and most of the results are still under evaluation, this section presents only some preliminary results at two gravel liquefaction sites (Sites 2 and 6, Petrinja) and at a sand liquefaction site with high fines content (Site 8, Donje Jame).

The energy transfer measurements at Site 6 indicate that the DPT hammer was providing an average of 89% of the theoretical free-fall energy, which is practically identical to the Chinese standard without requirement for hammer energy correction. Plots of the soil profile, the DPT blow count ( $N_{120}$ ), and the relative density are provided in Fig. 4. Preliminary analyses indicate that the friction on the drill rod behind the DPT cone artificially increased the  $N_{120}$  value in the clayey silt, while the CPT cone resistance remained essentially constant within similar materials. Therefore, the DPT blow counts below the clayey silt layer were corrected to account for this effect. Additional DPT testing is planned with an open borehole to the top of the gravel to confirm this correction. Using the corrected DPT blow counts in the sandy gravel to gravelly sand layers, correlations [29] indicate a relative density between 40 to 55%. These preliminary assessments indicate that the gravelly soil from about 4 to 6.25 m is the critical layer for liquefaction at this site. Ongoing mineralogical studies and liquefaction evaluations should help confirm this conclusion.

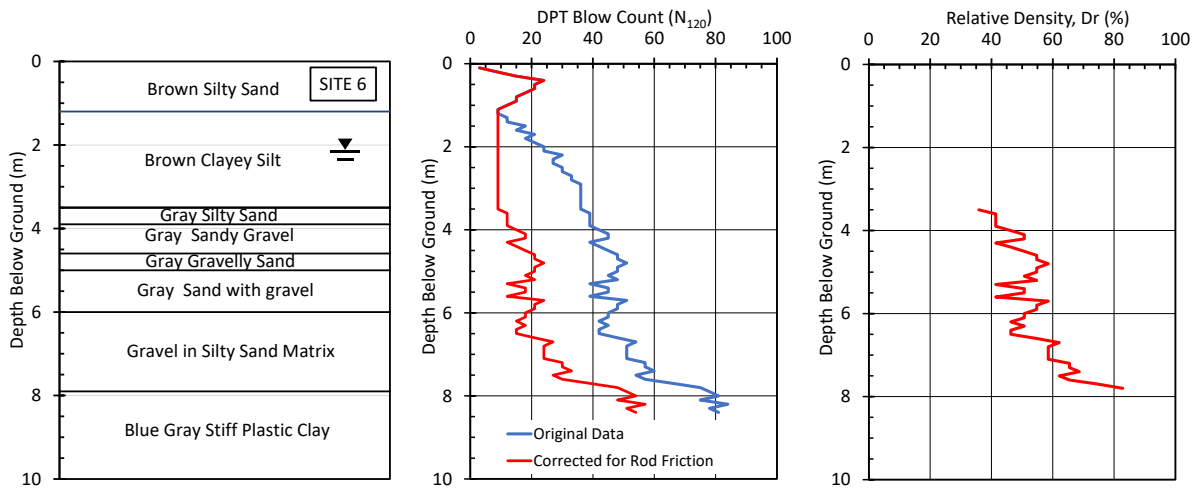


Figure 4. Preliminary DPT results for test site at Petrinja (Site 6).

At Site 8, a preliminary interpretation of the Medusa DMT was performed according to [30] correlations. Fig. 5 shows the DMT profiles in terms of: material index ( $I_D$ ) and the soil behaviour type index ( $SBT_{DMT}$ ) for the mechanical soil behaviour, constrained modulus ( $M$ ) for the soil stiffness at “operative” strain level, undrained shear strength ( $s_u$ ) and friction angle ( $\phi'$ ) for the soil resistance, and horizontal stress index ( $K_D$ ) for the stress history of the soil. The top 3.5 m are identified mostly as sands and silty sands, whereas silts, clayey and sandy silts are predominant at higher depths. This finding is in agreement with the borehole log and the CPTU data. According to the DMT and phreatimeter readings, the ground water table is located at 3 m depth, where the silty sandy layer is present. This body represents probably the one that liquefied during the Petrinja earthquake, as it was preliminary evaluated by examining the soil stratigraphy, the earthquake reconnaissance information and the  $K_D$  profile. However, liquefaction triggering analysis and laboratory tests on borehole samples and ejecta are required to confirm these preliminary outcomes.

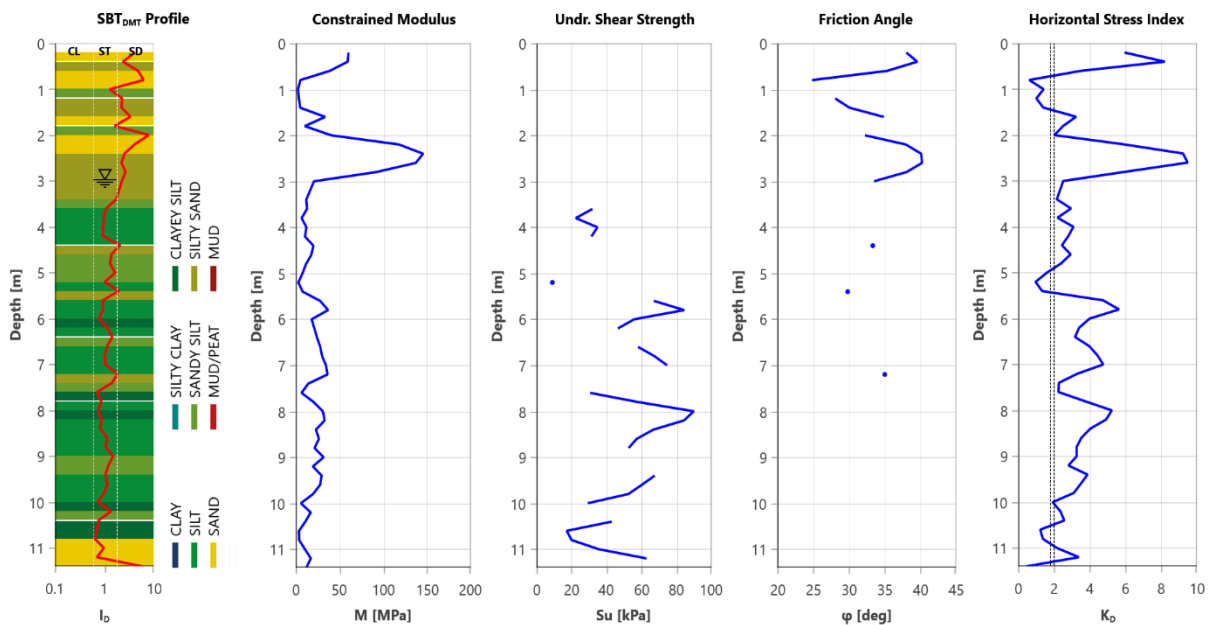


Figure 5. Preliminary Medusa SDMT results at the test site of Donje Jame (Site 8).

The objectives of the geophysical surveys were: (a) to infer the  $f_0$  value from the H/V curve (from 3C nodes); (b) to measure the surface-wave dispersion curve combining both passive and active array methods [31]; and (c) to infer the near-surface shear-wave velocity profile in the top few hundreds of meters by means of a joint inversion of the H/V and dispersion curves integrating results from geotechnical tests. Fig. 6 shows an example of the 2D array geometry applied in the field at two gravel sites in Petrinja (Sites 2 and 6), and the preliminary results in terms of H/V obtained at two arrays.

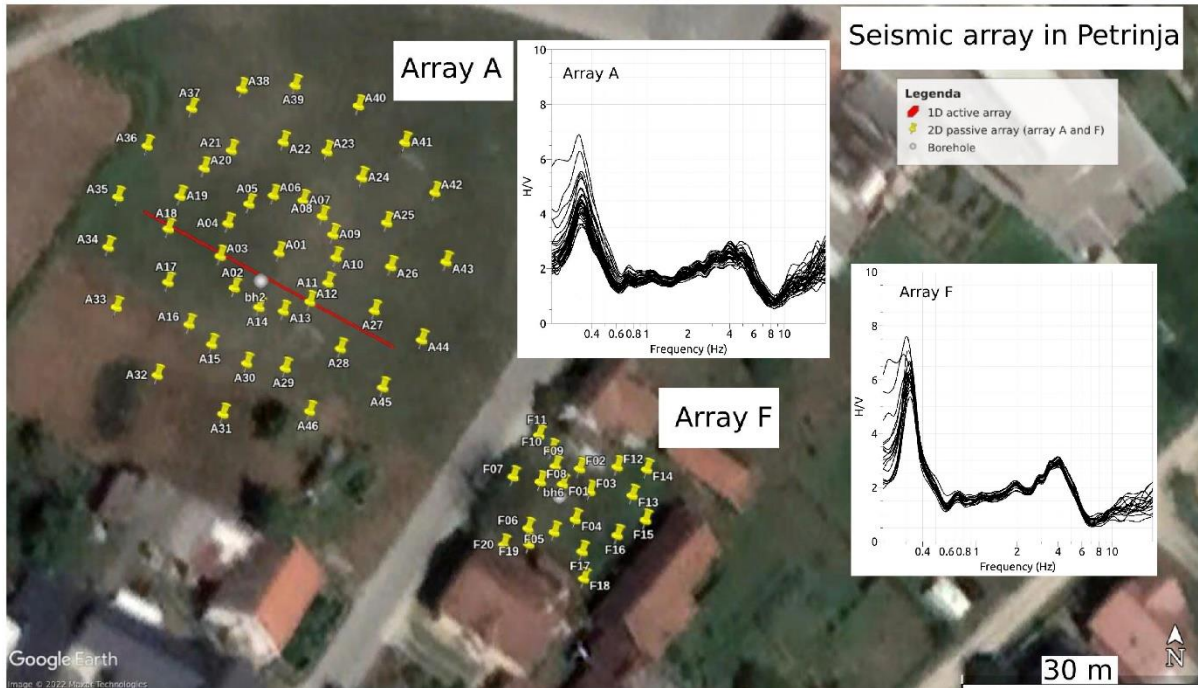


Figure 6. Seismic arrays in Petrinja. The yellow markers indicate the seismic nodes installed in 2D configuration (arrays A and F). The red line within array A shows the linear array of 72 geophones used for active experiment (the shot positions were situated at: -5 m and -2 m far from the first geophone, in the middle of the line, and at +2, +5, +10 m far from the last geophone). The mean H/V curves computed at all seismic nodes of the two arrays are also shown.

## 6. Conclusions

The 2020  $M_w$ 6.4 Petrinja earthquake offered the possibility for an in depth study of the liquefaction-induced features in the epicentral area. In particular, the variety of coseismic evidences (gravel liquefaction, lateral spreading and sand liquefaction with high fines content) provided an opportunity to improve knowledge of issues for which the experience is still limited.

In this respect, an intensive geological, geotechnical and geophysical campaign was planned at ten selected sites along the Kupa, Glina and Sava Rivers to verify the use of existing liquefaction triggering charts and to evaluate the soil properties of the liquefied layers and the non-liquefied crust. Some preliminary findings are reported in this paper based on extensive geophysical survey and two innovative geotechnical in-situ tests, the dynamic cone penetration test (DPT) and the Medusa flat dilatometer test (Medusa DMT). These results already provide a valuable information regarding the soil deposits that liquefied during the earthquake. Additional liquefaction triggering analysis and laboratory tests on borehole samples and ejecta are required to confirm these preliminary outcomes. More definitive conclusions should be possible once the ongoing field campaign and subsequent analyses are completed.



## Acknowledgements

Special thanks to Studio Prof. Marchetti for freely providing the Medusa seismic dilatometer equipment for the field investigations. This work is funded by Progetti di Ricerca Libera INGV 2021 (Istituto Nazionale di Geofisica e Vulcanologia) “Liquefaction Assessment of Gravelly Deposits (LAGD; 9999.816): historical data analyses and in situ testing at Italian trial sites to develop innovative methods”, by the Geotechnical Extreme Events Reconnaissance (GEER), by Brigham Young University (Provo, Utah) and by University of Ferrara (Ferrara, Italy). However, the opinions, conclusions, and recommendations in this paper do not necessarily represent those of the sponsors.

## References

- [1] Kramer, S.L. (1996). Geotechnical earthquake engineering. *Prentice Hall*, Upper Saddle River, N.J, 1996.
- [2] Baize, S., Amoroso, S., Belić, N., Benedetti, L., Boncio, P., Budić, M. Cinti, F.R., Henriquet, M., Jamšek Rupnik, P., Kordić, B., Markušić, S., Minarelli, L., Pantosti, D., Pucci, S., Špelić, M., Testa, A., Valkaniotis, S., Vukovski, M., Atanackov, J., Barbača, J., Bavec, M., Brajković, R., Brčić, V., Caciagli, M., Celarc, B., Civico, R., De Martini, P.M., Filjak, R., Iezzi F., Moulin, A., Kurečić, T., Métois, M., Nappi, R., Novak, A., Novak, M., Pace, B., Palenik, D. and Ricci T. (2022). Environmental effects and seismogenic source characterization of the December 2020 earthquake sequence near Petrinja, Croatia. *Geophysical Journal International* **230**(2): 1394–1418. <https://doi.org/10.1093/gji/ggac123>
- [3] Amoroso, S., Barbača, J., Belić, N., Kordić, B., Brčić, V., Budić, M., Civico, R., De Martini, P.M., Hećej, N., Kurečić, T., Minarelli, L., Novosel, T., Palenik, D., Pantosti, D., Pucci, S., Filjak, R., Ricci, T., Špelić, M. and Vukovski, M. (2021). Liquefaction field reconnaissance following the 29th December 2020 Mw 6.4 Petrinja earthquake (Croatia). *Proc. EGU General Assembly 2021, online*; 19–30 Apr 2021, Abstract No. EGU21-16584. <https://doi.org/10.5194/egusphere-egu21-16584>
- [4] Pollak, D., Gulam, V., Novosel, T., Avanić, R., Tomljenović, B., Hećej, N., Terzić, J., Stipčević, J., Bačić, M. and Kurečić, T. (2021). The preliminary inventory of coseismic ground failures related to December 2020 – January 2021 Petrinja earthquake series. *Geologia Croatica: Journal of the Croatian Geological Survey and the Croatian Geological Society* **74**(2): 189-208. <https://doi.org/10.4154/gc.2021.08>
- [5] Schmid, S.M., Fügenschuh, B., Kounov, A., Maženco, L., Nievergelt, P., Oberhänsli, R., Pleuger, J., Schefer, S., Schuster, R., Tomljenović, B., Ustaszewski, K. and van Hinsbergen, D.J.J. (2020). Tectonic units of the Alpine collision zone between Eastern Alps and western Turkey. *Gondwana Research* **78**: 308–374. <https://doi.org/10.1016/j.gr.2019.07.005>
- [6] Tomljenović, B. and Csontos, L. (2001). Neogene–Quaternary structures in the border zone between Alps, Dinarides and Pannonian Basin (Hrvatsko zagorje and Karlovac Basins, Croatia). *International Journal of Earth Sciences* **90**: 560–578. <https://doi.org/10.1007/s005310000176>
- [7] Ustaszewski, K., Kounov, A., Schmid, S.M., Schaltegger, U., Krenn, E., Frank, W. and Fügenschuh, B. (2010). Evolution of the Adria-Europe plate boundary in the northern Dinarides: From continent-continent collision to back-arc extension: Adria-Europe Plate Boundary, Dinarides. *Tectonics* **29**. <https://doi.org/10.1029/2010TC002668>
- [8] Pikija, M. (1987). Basic Geological Map of SFRY 1:100.000, Sisak sheet. *Geol. Zavod, Zagreb, Savezni geol. Zavod, Beograd* [in Croatian].
- [9] Šikić, K. (2014). Basic Geological Map of Republic Croatia 1:100.000, Bosanski Novi sheet. *Croatian Geological Survey, Zagreb* [in Croatian].
- [10] Pavelić, D. and Kovačić, M. (2018). Sedimentology and stratigraphy of the Neogene rift-type North Croatian Basin (Pannonian Basin System, Croatia): A review. *Marine and Petroleum Geology* **91**: 455–469. <https://doi.org/10.1016/j.marpetgeo.2018.01.026>
- [11] Markušić, S., Stanko, D., Penava, D., Ivančić, I., Bjelotomić Oršulić, O., Korbar, T. and Sarhosis, V. (2021). Destructive M6.2 Petrinja Earthquake (Croatia) in 2020—Preliminary Multidisciplinary Research. *Remote Sensing* **13**: 1095. <https://doi.org/10.3390/rs13061095>
- [12] Herak, M., Herak, D. and Markušić, S. (1996). Revision of the earthquake catalogue and seismicity of Croatia, 1908–1992. *Terra Nova* **8**: 86–94.

- [13] Chinese Design Code (2001). Design code for building foundation of Chengdu region. *Administration of Quality and Technology supervision of Sichuan Province PRC DB51/T5026-2001* [in Chinese].
- [14] Chinese Specifications 1999. Specification of soil test. *Ministry of Water Resources of the People's Republic of China SL237-1999* [in Chinese].
- [15] Cao, Z., Youd, T.L. and Yuan, X. (2011). Gravelly soils that liquefied during 2008 Wenchuan, China Earthquake, Ms=8.0. *Soil Dynamics and Earthquake Engineering* **31**: 1132-1143.
- [16] Rollins, K.M., Roy, J., Athanasopoulos-Zekkos, A., Zekkos, D., Amoroso, S. and Cao, Z. (2021). A new dynamic cone penetration test-based procedure for liquefaction triggering assessment of gravelly soils. *Journal of Geotechnical and Geoenvironmental Engineering* **147**(12): 04021141. [https://doi.org/10.1061/\(ASCE\)GT.1943-5606.0002686](https://doi.org/10.1061/(ASCE)GT.1943-5606.0002686)
- [17] Marchetti, D. (2018). Dilatometer and Seismic Dilatometer Testing Off-shore: Available Experience and New Developments. *Geotechnical Testing Journal* **41**(5): 967–977. <https://doi.org/10.1520/GTJ20170378>
- [18] Marchetti, D., Monaco, P., Amoroso, S. and Minarelli, L. (2019). In situ tests by Medusa DMT. *Proc. XVII European Conference on Soil Mechanics and Geotechnical Engineering*; Reykjavik, Iceland, 2019, 1–8. <https://doi.org/10.32075/17ECSMGE-2019-0657>
- [19] Monaco, P., Marchetti, D., Totani, G., Totani, F. and Amoroso, S. (2022). Validation of Medusa DMT test procedures in Fucino clay. *Proc. 20th International Conference on Soil Mechanics and Geotechnical Engineering*; 1-5 May 2022, Sydney, Australia, 471-476.
- [20] Monaco, P., Tonni, L., Amoroso, S., Martinez, M.F., Gottardi, G., Marchetti, D. and Minarelli L. (2021). Use of Medusa DMT in alluvial silty sediments of the Po river valley. *Proc. 6th International Conference on Geotechnical and Geophysical Site Characterization - ISC'6 Conference*; 26-29 September 2021, Budapest, Hungary.
- [21] Dean, T., Tulett, J. and Barnwell, R. (2018). Nodal land seismic acquisition: The next generation. *First Break* **36**(1): 47-52.
- [22] Dean, T. and Sweeney, D. (2019). The use of nodal seismic acquisition systems to acquire limited-scale surveys. *First Break* **37**(1): 55-60.
- [23] Molnar, S., Cassidy, J.F., Castellaro, S., Cornou, C., Crow, H., Hunter, J.A., Matsushima, S., Sánchez-Sesma, F.J. and Yong, A. (2018). Application of microtremor horizontal-to-vertical spectral ratio (MHVSR) analysis for site characterization: State of the art. *Surveys in Geophysics* **39**(4): 613-631.
- [24] Di Giulio, G., Cultrera, G., Cornou, C., Bard, P.Y. and Al Tfaily, B. (2021). Quality assessment for site characterization at seismic stations. *Bulletin of Earthquake Engineering* **19**(12): 4643-4691.
- [25] Bonnefoy-Claudet, S., Cornou, C., Bard, P.Y., Cotton, F., Moczo, P., Kristek, J. and Fäh, D. (2006). H/V ratio: A tool for site effects evaluation. Results from 1-D noise simulations. *Geophysical Journal International* **167**(2): 827-837.
- [26] Park, C. B., Miller, R. D., Xia, J. and Ivanov, J. (2007). Multichannel analysis of surface waves (MASW)- Active and passive methods. *The Leading Edge* **26**: 60-64
- [27] Wathelet, M., Guillier, B., Roux, P., Cornou, C. and Ohrnberger, M. (2018). Rayleigh wave three-component beamforming: signed ellipticity assessment from high-resolution frequency-wavenumber processing of ambient vibration arrays. *Geophysical Journal International* **215**(1): 507-523.
- [28] Foti, S., Lai, C.G., Rix, G.J. and Strobbia, C. (2015). *Surface Wave Methods for Near-Surface Site Characterization*, CRC press.
- [29] Rollins, K.M., Amoroso, S., Milan, G., Minerelli, L., Vassallo, M. and Di Giulio, G. (2020). Gravel liquefaction assessment using the dynamic cone penetration test based on field performance from the 1976 Friuli earthquake. *Journal of Geotechnical and Geoenvironmental Engineering* **146**(6): 04020038 [https://doi.org/10.1061/\(ASCE\)GT.1943-5606.0002252](https://doi.org/10.1061/(ASCE)GT.1943-5606.0002252)
- [30] Marchetti, S., Monaco, P., Totani, G. and Calabrese, M. (2001). The Flat Dilatometer Test (DMT) in Soil Investigations – A Report by the ISSMGE Committee TC16. *Proc. International Conference on In situ Measurement of Soil Properties and Case Histories*; Bandung, Indonesia, 2001, 95–131. Official version approved by TC16 reprinted *Proc. 2nd International Conference on the Flat Dilatometer*; Washington D.C., USA, 2006, 7–48.

- [31] Wathelet, M., Chatelain, J.L., Cornou, C., Giulio, G.D., Guillier, B., Ohrnberger, M. and Savvaidis, A. (2020). Geopsy: A user - friendly open - source tool set for ambient vibration processing. *Seismological Research Letters* **91**(3): 1878-1889.